Representing Indian Agricultural Practices and Paddy Cultivation in the Variable Infiltration Capacity Model

Jisha Joseph[1] and Subimal Ghosh[1]

[1]Indian Institute of Technology Bombay

November 21, 2022

Abstract

Increased irrigation due to agricultural intensification has profound impacts on the surface water and energy balance at regional to local scales. Recent updates of the state of the art Land Surface Models (LSMs) include the impacts of irrigation on surface hydrology. The Indo-Gangetic Plain (IGP) is one of the global hotspots of irrigation water applications. However, the direct application of these models to Indian basins has certain limitations. The commonly employed flood irrigation technique is often indiscriminate and unmanaged, unlike the state-of-the-art models' estimation of crop water use based on soil moisture conditions. The primary crop in the IGP is paddy, cultivated in inundated fields with quite distinct water and energy partitioning mechanisms represented in very few models. Here, we developed an improved irrigation module to simulate the Indian agricultural practices for the widely used Variable Infiltration Capacity (VIC) model. We incorporated the crop-specific water use for flood irrigation, calculated based on previously reported field studies. The water and energy balance processes are modified by incorporating the ponded paddy fields with proper parameterization. We achieved a substantial improvement in the simulated evapotranspiration and soil moisture of the IGP, particularly in the non-monsoon seasons with the updated model. We found that evapotranspiration and soil moisture are more sensitive to the irrigation techniques than the interval of irrigation application. Runoff strongly responded to irrigation technique as well as the interval of application. We emphasize accurate representation of irrigation practices in the LSMs, specifically when applied to the human-natural hydrological system.

Hosted file

`supporting information_18_10_2021.docx` available at https://authorea.com/users/531139/articles/597561-representing-indian-agricultural-practices-and-paddy-cultivation-in-the-variable-infiltration-capacity-model

Hosted file

`essoar.10508440.1.docx` available at https://authorea.com/users/531139/articles/597561-representing-indian-agricultural-practices-and-paddy-cultivation-in-the-variable-infiltration-capacity-model

Representing Indian Agricultural Practices and Paddy Cultivation in the Variable Infiltration Capacity Model

Jisha Joseph[1] and Subimal Ghosh[1,2,*]

[1]Department of Civil Engineering, Indian Institute of Technology Bombay, Mumbai, India, [2]Interdisciplinary Program in Climate Studies, Indian Institute of Technology Bombay, Mumbai, India.

[*]**Correspondence to:** Subimal Ghosh, subimal@civil.iitb.ac.in

Key Points

- Formulation of a new irrigation module suitable for India representing unrestrained agricultural water use and submerged paddy fields
- Improved simulations of evapotranspiration and soil moisture by the developed model
- Technique and interval of irrigation influences evapotranspiration, soil moisture, and runoff

Abstract

Increased irrigation due to agricultural intensification has profound impacts on the surface water and energy balance at regional to local scales. Recent updates of the state of the art Land Surface Models (LSMs) include the impacts of irrigation on surface hydrology. The Indo-Gangetic Plain (IGP) is one of the global hotspots of irrigation water applications. However, the direct application of these models to Indian basins has certain limitations. The commonly employed flood irrigation technique is often indiscriminate and unmanaged, unlike the state-of-the-art models' estimation of crop water use based on soil moisture conditions. The primary crop in the IGP is paddy, cultivated in inundated fields with quite distinct water and energy partitioning mechanisms represented in very few models. Here, we developed an improved irrigation module to simulate the Indian agricultural practices for the widely used Variable Infiltration Capacity (VIC) model. We incorporated the crop-specific water use for flood irrigation, calculated based on previously reported field studies. The water and energy balance processes are modified by incorporating the ponded paddy fields with proper parameterization. We achieved a substantial improvement in the simulated evapotranspiration and soil moisture of the IGP, particularly in the non-monsoon seasons with the updated model. We found that evapotranspiration and soil moisture are more sensitive to the irrigation techniques than the interval of irrigation application. Runoff strongly responded to irrigation technique as well as the interval of application. We emphasize accurate representation of irrigation practices in the LSMs, specifically when applied to the human-natural hydrological system.

Plain Language Summary

Irrigation has a substantial impact on the water and energy cycle at a local scale.

The water from surface and ground repositories is redistributed over the croplands, thereby enhancing evaporation, cooling the soil surface, and modifying spatiotemporal precipitation patterns. Therefore, regional hydrological modelling is incomplete without incorporating farming practices in an agriculture-dominated country like India, with vast croplands and extensive irrigation. Traditionally, the irrigation scheme in existing models calculates the daily water demand of the crop on the basis of the moisture content of the soil. However, readily available groundwater and subsidized electricity for its abstraction have led to unmanaged irrigation exceeding the crop demand. Paddy, widely cultivated in India, has distinctive mechanisms for water and energy partitioning. Thus, we have developed a more pragmatic irrigation scheme with submerged paddy fields and user-specified irrigation water applications. We tested the model over widely irrigated Indo-Gangetic Plain (IGP) and noted good performance in estimating the seasonal soil moisture and evapotranspiration. We also found that the irrigation mode and frequency of water application affect soil moisture, evaporation, and runoff. We emphasize accurate representation of irrigation activities to precisely estimate their effects on a regional scale.

1. Introduction

Global cropland has expanded rapidly from 1.35 billion hectares in the 1960s to 1.55 billion hectares in the 2010s, though the rise is marginal from the 2000s (World Food and Agriculture-Statistical Yearbook, 2020). The irrigated area has also grown significantly post Green Revolution, notably in South Asia (Foley et al., 2011; Shukla et al., 2014; Siebert et al., 2015). This rise is attributed to the burden posed on food production due to the growing population (Davis et al., 2018; Godfray et al., 2010). Besides, climate-induced warming and precipitation variability have led to further irrigation reliance (Döll, 2002; Lal, 2011; Rajagopalan et al., 2018). Irrigation buffers the sensitivity of crops to climate variability (Li & Troy, 2018). The largest share of the global cropland area comes from India (World Food and Agriculture-Statistical Yearbook, 2020). It has also witnessed substantial expansion in the irrigated area from 28 million hectares in the 1960s to 70 million hectares in the 2010s (Agricultural statistics at a glance, 2018). Increased cereal cultivation, specifically rice during monsoon and wheat during the winter season, has played a vital role in increasing irrigation water use in India (Davis et al., 2018).

Drastic transition to croplands and irrigation intensification have influenced the regional climate by altering the water and energy cycle (Foley et al., 2005; Portmann et al., 2010; Puma & Cook, 2010; Rockström et al., 2009). At a local scale, irrigation raises the moisture content of the soil, leading to increased evapotranspiration (ET) (Szilagyi & Jozsa, 2018; Zou et al., 2017) and decreased surface temperature(Chen et al., 2018; Tatsumi & Yamashiki, 2015; Thiery et al., 2017; Yang et al., 2020). Thiery et al. (2017,2020) suggested an alleviation in heat extremes due to irrigation induced cooling, though unintended. Few studies reported irrigation initiated improved precipitation and runoff at a regional scale (Lo & Famiglietti, 2013; Wei et al., 2013; Zhang et al., 2017). The partitioning of energy at the surface gets affected by the changes in soil moisture (SM). Sensible heat flux declines, and latent heat flux rises in irrigated regions(Chen et al., 2018; Kueppers & Snyder, 2012; Tatsumi & Yamashiki, 2015; Zou et al., 2017). The altered energy regime influences the boundary layer formation (E. M. Douglas et al., 2009; Ellen M. Douglas et al., 2006). In some of the basins, the influences of agricultural and irrigation activities on the water cycle were more compared to climate change (Ingjerd Haddeland et al., 2014; Jaramillo & Destouni, 2015; Leng et al., 2015a; Zou et al., 2017).

In India, a rise in latent heat fluxes (Ellen M. Douglas et al., 2006; de Rosnay et al., 2003), increased vapour fluxes, modifications in spatial and temporal patterns of precipitation (Chou et al., 2018; Niyogi et al., 2010; Saeed et al., 2009; Shukla et al., 2014), reduced sensible heat fluxes, lowered planetary boundary layer(Mishra et al., 2020), and surface cooling (Douglas et al., 2009) attributable to irrigation were reported. Guimberteau et al. (2012) suggested a delay in the onset of monsoon and decreased precipitation due to irrigation activities. Simulations performed by Devanand et al. (2019) revealed that monsoon rainfall also depends on the mode of irrigation application. Hence, the need of accurate representation of irrigation activities cannot be ignored in hydroclimatic modelling, particularly in regions with considerable human interventions (Haddeland et al., 2014; Jaramillo & Destouni, 2015).

Recently, there have been significant advancements in incorporating irrigation practices in land surface models. WaterGAP (Water-Global Assessment and Prognosis) model was among the earliest models developed to calculate the irrigation water use based on precipitation reaching the ground and potential ET of crops(Alcamo et al., 2003; Döll et al., 2003). de Rosnay et al. (2003) added an irrigation scheme to ORCHIDEE (Organizing Carbon and Hydrology In Dynamic EcosystEms) LSM and calculated the irrigation demand based on potential ET from FAO guidelines. An integrated model named H08 with six modules for water balance, routing of river discharge, crop growth, reservoir operation, estimation of environmental flow, and human water use was developed by Hanasaki et al. (2008a,b). The water required to raise the SM to 75% of field capacity was considered the irrigation demand. Later, Pokhrel et al. (2012) incorporated the anthropogenic water use component of H08 to the Minimal Advanced Treatments of Surface Interaction and Runoff (MATSIRO) model. Studies on coupling irrigation schemes to LSMs like Noah (Sorooshian et al., 2014) and CLM (Leng et al., 2014, 2015) have also been performed. Leng et al. (2014) parametrized irrigation scheme into Accelerated Climate Modeling for Energy (ACME) Land Model (ALM) and evaluated the sensitivity of water fluxes on different modes of irrigation application and source of water abstraction.

Variable Infiltration Capacity (VIC) Model is a widely used model for Indian river basins (Chandel & Ghosh, 2021; Chawla & Mujumdar, 2015; Ghosh et al., 2016; Niroula et al., 2018; Raje et al., 2014; Saha et al., 2020). Haddeland et al. (2006 a;b) developed an irrigation module for VIC. The formulations represent a sprinkler irrigation scheme, with irrigation application based on the moisture content of the soil. When the SM dropped below a critical value under which transpiration is limited, irrigation was added to the precipitation reaching the ground until the soil field capacity was attained. This module can either estimate the irrigation water demand irrespective of availability or actual irrigation where water is extracted from the nearest river or reservoir based on water availability. This irrigation module has been applied over various river basins, and an increase in latent heat flux and decrease in surface temperature over irrigated grids were reported (Chen et al., 2018; Tatsumi & Yamashiki, 2015). Droppers et al. (2020) developed VIC-WUR (Wageningen University and Research), which comprises VIC coupled with additional modules like irrigation, dam operation, and groundwater pumping from the bottom soil layer to represent human interactions in land surface modelling. In few studies, agricultural models have been coupled to VIC to better estimate irrigation water demands by simulating crop growth (Malek et al., 2017; Rajagopalan et al., 2018).

Although extensively irrigated, hydroclimatic studies incorporating irrigation over India are limited. de Rosnay et al. (2003) employed the irrigation coupled ORCHIDEE (Organizing Carbon and Hydrology In Dynamic EcosystEms) model over Indian Peninsula and observed a strong positive correlation between latent heat flux and the amount of irrigation applied. Shah et al. (2019) used the VIC irrigation module to estimate irrigation water demands over Indian river basins. They investigated the effects of irrigation application and found an increase in ET and total runoff. Irrigation demands were based on the SM and hence showed a correlation to the monsoon rainfall. Shah et al. (2019) further simulated constrained irrigation scenarios in India by including VIC-reservoir module with surface water as the only source. They concluded that ET during pre-monsoon and post-monsoon has increased as a consequence of irrigation. However, constrained irrigation resulted in lesser mean annual ET when compared to potential irrigation, where water availability is unlimited. Similarly, H. Xie et al. (2020) added a groundwater-fed irrigation module into the SWAT (Soil and Water Assessment Tool) model based on soil-moisture conditions to study the groundwater trends over India.

However, the irrigation scenario in India is quite different. Conventional flood irrigation, which has poor efficiency, is the most common mode of water application (Barik et al., 2017). Variability and weakening of monsoon precipitation have resulted in the dependence on groundwater to meet agricultural demands(Asoka et al., 2017). Unmetered groundwater and subsidies on electricity for pumping encouraged farmers to abstract excess amounts of water and flood the fields in an uncontrolled manner (Devineni et al., 2013; Fishman et al., 2015; Vatta et al., 2018; Zaveri et al., 2016). Hence, irrigation water use in India is far from demand-driven and underestimated in existing irrigation coupled hydrological models. Data corresponding to the amount and frequency of water application is scarce (O'Keeffe et al., 2018). It is also noteworthy that paddy is one of the significant Kharif crops and is cultivated under ponded conditions. The water balance and energy partitioning under submerged conditions are different. Only a few models have incorporated paddy formulations (Devanand et al., 2019; Masutomi et al., 2016; Tsuchiya et al., 2016; Xie & Cui, 2011). Multiple cropping seasons and myriad crop varieties are yet another feature and need to be addressed in irrigation coupled hydrological models. These limitations emphasize the call for designing an irrigation module specifically for India for more realistic representations. Here we develop a new irrigation module integrated into the VIC model suitable for the Indian irrigation scenario. This module adds crop-specific water use for flood irrigation to the precipitation reaching the surface. The water and energy processes of paddy fields are handled separately. The irrigation water can be applied at daily or weekly intervals. Additionally, we performed a simulation employing drip irrigation scheme parametrized into the VIC model to compare the effects of different irrigation techniques. The detailed flow diagram is represented in Figure 1. The study's objectives include a) to develop an irrigation model for VIC representing Indian irrigation practices; b) to apply the developed model to the IGP, one of the global irrigation hotspots; c) to compile crop area, irrigated area, and irrigation water use data for IGP from different available sources and Government data; d) to evaluate the newly developed model with flood irrigation and paddy formulations for the hydrologic simulations in the IGP; and e) to assess the sensitivity of ET, SM, and runoff on the mode and frequency of irrigation application.

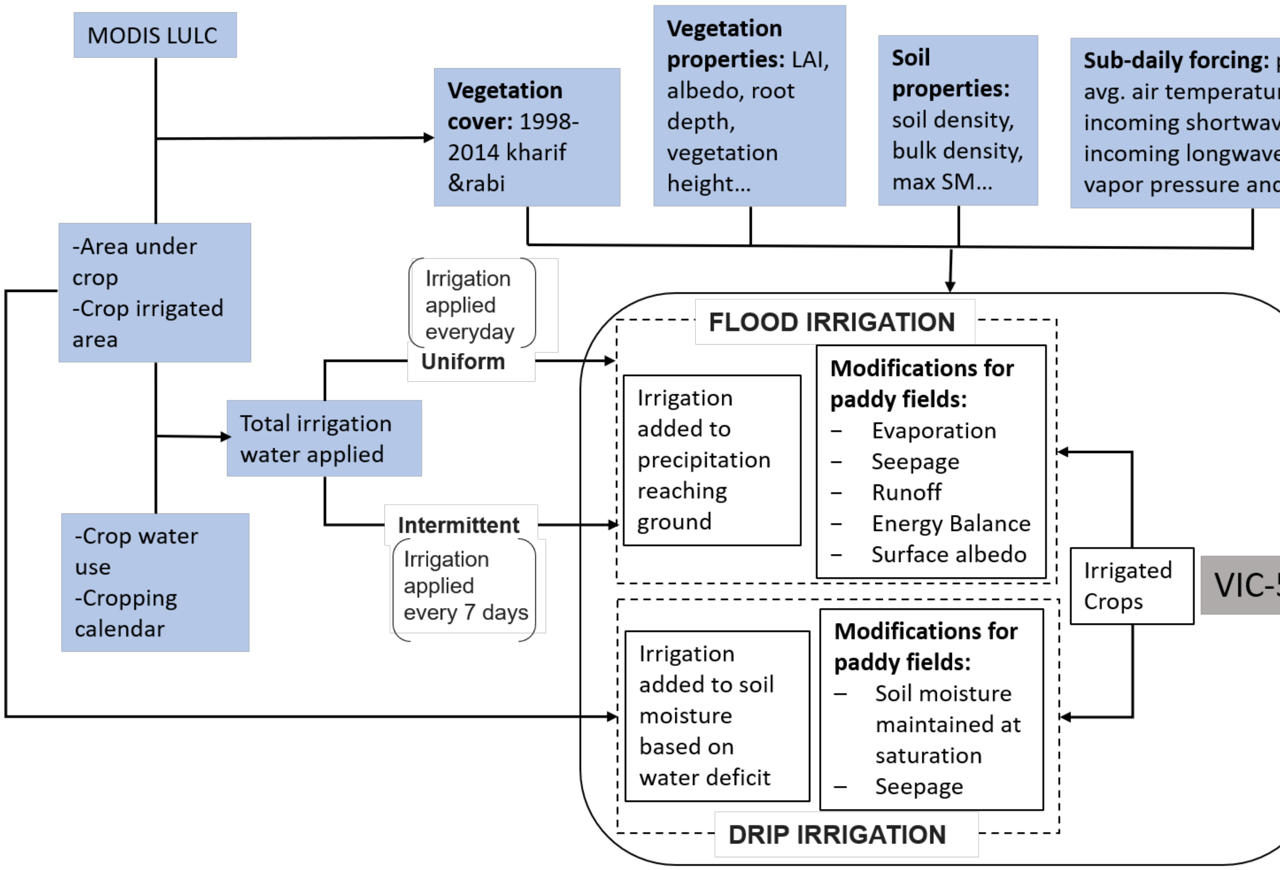

Figure 1. Flow diagram depicting the methodology followed.

2. Study Area and Data Used

2.1 Study Area

India is the most significant contributor to global cropland. In 2018, its share was reported to be 11% of the total encompassing over 140 million hectares of cropland. Almost 90% of the total water withdrawn is utilized for agriculture (World Food and Agriculture-Statistical Yearbook, 2020). India has mainly three cropping seasons: Kharif roughly from June to October overlapping the monsoon season, Rabi during winter spanning from November to February and Zaid during summer months of March to May. Principal crops cultivated include cereals (rice, jowar, bajra, maize, wheat and barley), pulses (gram and tur/arhar), sugarcane, oilseeds (groundnut, soyabean, mustard and sunflower), cotton, and tobacco (Agricultural statistics at a glance, 2018). Cereals, specifically rice and wheat, dominate in terms of percentage share to croplands. Here, we focus on the major part of the IGP region covering Punjab, Haryana, Delhi, and Rajasthan in the northwest, Uttar Pradesh and Bihar in the central IGP, and a few districts of Uttarakhand, Madhya Pradesh, Chhattisgarh, and Jharkhand (Figure 2a). The dominant land cover type is cropland (Figure 2b and 2c) and is extensively irrigated. Barik et al. (2017) listed these states among the key producers of cereal crops. Rainfall during monsoon, perennial rivers, fertile soil predominantly alluvial (in Punjab, Haryana, Uttar Pradesh, and Bihar), and anytime accessible groundwater makes this region arable, with western Rajasthan as an exception. During the Kharif season, the fraction of rainfed crops is more. Rice followed by sugarcane and cotton are prevalent among irrigated crops (Figure 2d). Wheat, sugarcane, and gram are the key crops in the Rabi season, with a lesser fraction of rainfed crops (Figure 2e).

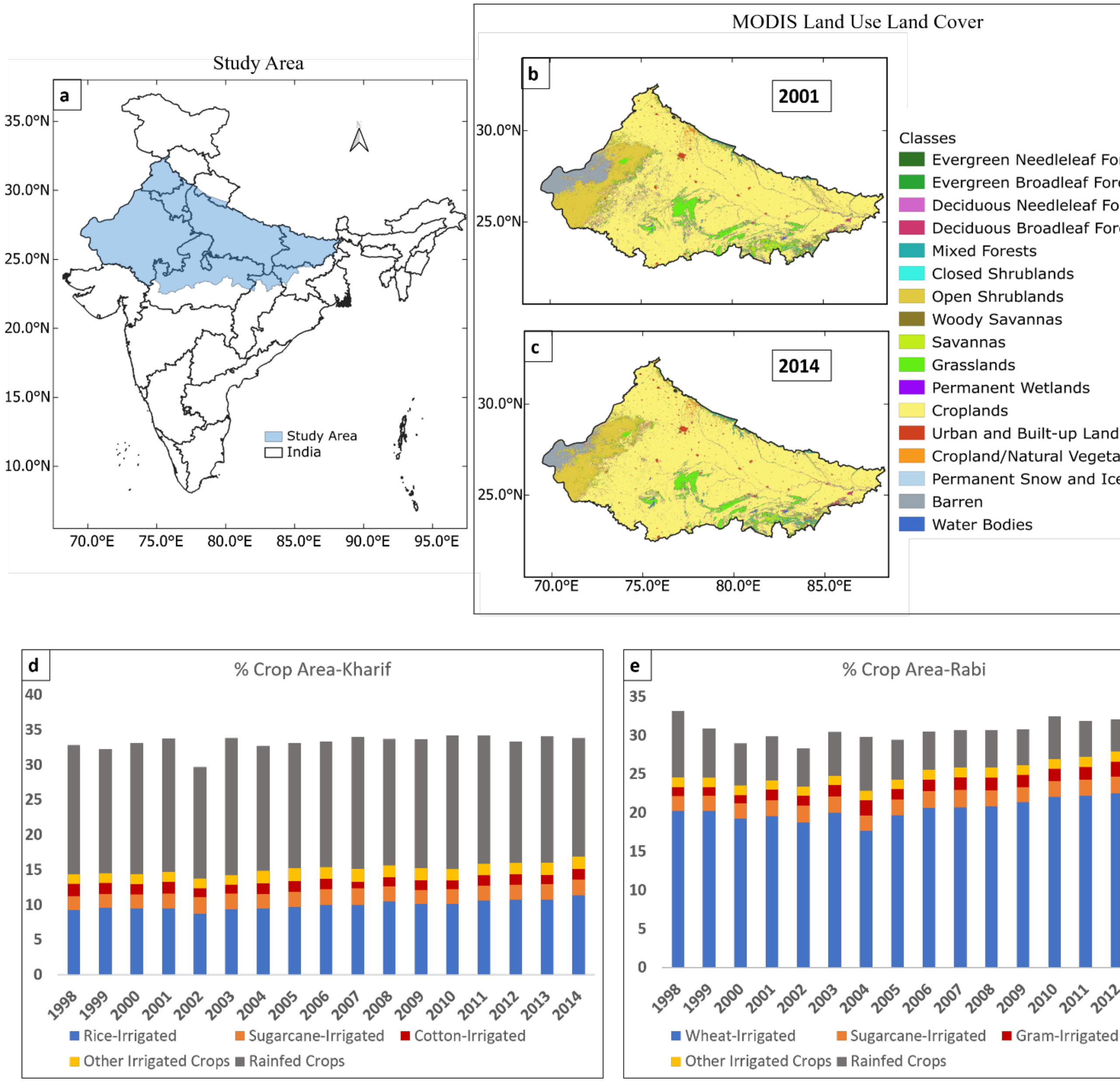

Figure 2. (a)Geographical location of the study area in India represented by blue shaded region. MODIS LULC with IGBP classification scheme for 2001(b) and 2014(c) showing the extent of croplands. Percentage of crop area for the period 1998-2014 with shares of rainfed and key irrigated crops for (d) Kharif season and (e) Rabi season.

2.2 Data Used

2.2.1 Input data for VIC model

The meteorological inputs required for running VIC version 5 (the most recent version) include average air temperature, total precipitation (rain and snow), atmospheric pressure, incoming shortwave radiation, incoming longwave radiation, vapour pressure and wind speed at a sub-daily time step. As a preprocessing step to generate these sub-daily forcings, VIC-4.2.d was executed. This version of VIC uses Mountain Microclimate Simulation Model (MTCLIM) (Bohn et al., 2013) as a meteorological forcing generator and disaggregates them to sub-daily time step. Observed precipitation, minimum and maximum temperature, and wind speed at a daily scale were given as inputs. Indian Meteorological Department (IMD) provides gridded data products for observed precipitation at 0.5° and 0.25° resolution and temperature at 1° resolution. The gridded rainfall data are obtained by interpolating daily observation from over 3000 gauge stations in India (Rajeevan et al., 2006; Rajeevan & Bhate, 2009). For gridded temperature data, interpolation is performed based on 395 gauge stations (Srivastava et al., 2009). Wind data was procured from European Centre for Medium-Range Weather Forecasts (ECMWF) interim reanalysis (ERA-Interim). ERA-Interim data is developed by assimilating observation fields to a forecast model using four-dimensional variational assimilation system (4D-Var). All the forcing inputs were regridded to 0.5°, and VIC-4.2.d was implemented. The outputs included all the forcing at a 6-hourly time step needed to run VIC-5.

Additionally, VIC requires soil properties, vegetation properties, and land use land cover details. Soil properties like bulk density, soil density, hydraulic conductivity, etc., are procured from global soil input parameters available at the VIC website. The soil parameter was originally prepared using Food and Agricultural Organisation (1995) soil map at 2° resolution (Nijssen et al., 2001a;b). This soil file was regridded to 0.5° resolution using the nearest neighbourhood approach and is freely available at the VIC website (https://vic.readthedocs.io/en/master/Datasets/Datasets/#vic-input-and-output-data-sets). The fractional vegetation cover was calculated using Moderate Resolution Imaging Spectroradiometer (MODIS) satellite-based land cover type (Sulla-Menashe et al., 2019). The land cover data is at 0.05° spatial resolution and available at yearly time step from 2001-2019. Six land use classification schemes comprising of IGBP land cover classification, University of Maryland (UMD), Biome classification scheme, LAI/fPAR Biome scheme and Plant Functional Type scheme are included in the data product. IGBP classification scheme was selected for the present analysis. The vegetation properties like LAI, albedo, root depth, vegetation height for all the vegetation classes except croplands were collected from Global Land Data Assimilation (GLDAS) vegetation parameters. The procedures followed for irrigation data preparation are explained in the next section.

ET simulated from model runs was evaluated using Global Land Evaporation Amsterdam Model (GLEAM) v3.5 ET(Martens et al., 2017). GLEAM comprises different algorithms that make use of satellite data to calculate ET and root zone SM. Using Vertical Optical Depth (VOD) from observations and root zone SM, evaporative stress factors are calculated. Potential ET estimated using Priestley and Taylor equation is multiplied with the evaporative stress factor to obtain actual ET. GLEAM ET showed a good correlation when compared against eddy covariance towers, globally. GLEAM ET data can be obtained at monthly time step from 1980 to 2020 at 0.25° resolution. European Space Agency Climate Change Initiative (ESA CCI) for SM v06.1(Dorigo et al., 2017; Gruber et al., 2019) was used for SM validation. This data is available at a spatial resolution 0f 0.25° and spans over 1978-2020.

2.2.2 Data for irrigation scheme

Data required for the irrigation scheme include crop-wise area, the fraction of irrigated and rainfed crops, vegetation properties, crop-specific water use and crop calendar. The Crop Production Statistics Information System by the Directorate of Economics and Statistics provides district-wise Area under Crop (AUC) and Crop Irrigated Area (CIA) from 1998-1999 (https://aps.dac.gov.in/LUS). We have focused on ten major crops grown in the Kharif season: Rice, Jowar, Maize, Bajra, Tur, Sugarcane, Cotton, Tobacco, Groundnut, and Soyabean. We used several Rabi season crops, including Rice, Maize, Barley, Sugarcane, Gram, Wheat, Jowar, and Tobacco. Sugarcane is grown around the year. Due to inconsistencies in crop area data from multiple sources, we have not considered summer (Zaid) crops. The cultivation during the Zaid season is also small compared to other seasons. Based on field experience, Fishman et al. (2015) have documented water use of major crops under flood irrigation during the growing season (Supplementary Table S1). The total amount of irrigation applied for a specific crop is calculated by multiplying water use with its CIA. Previous studies have reported vegetation properties like LAI (Balakrishnan et al., 1987; Bandyopadhyay et al., 2010; Boken & Chandra, 2012; Gadi et al., 2016; Garg et al., 2014; Ghule et al., 2013; Gomathi et al., 2013; Kour et al., 2016; Rao et al., 2006; Reddy & Willey, 1981; Shankar et al., 2012; Sood et al., 2006; Verma et al., 2016; Zhengyang et al., 2011), albedo (Bsaibes et al., 2009), vegetation height (Konlan et al., 2013; Srichandan & Mangaraj, 2015) and root depth (Fan et al., 2016; Shankar et al., 2012; Siebert & Döll, 2010) of crops, at various growth stages, derived from field and satellite observations. We have compiled monthly vegetation properties based on these findings. Crop calendar data comprising the information on sowing and harvesting months were prepared by the Indian Council of Agricultural Research and obtained from the Directorate of Economics and Statistics website (https://eands.dacnet.nic.in/At_A_Glance-2011/Appendix-IV.xls).

We have selected a simulation period of 17 years from 1998 to 2014 on account of data availability. Gridded fractions of land cover type are estimated using MODIS LULC data available at yearly timestep from 2001. We have used the LULC map of 2001 for 1998-2000 as well. The district-wise AUC and CIA are interpolated to the model grids. Within each grid, cropland areas from MODIS LULC (C_{MODIS}) are compared to the sum of the AUC of all the crops for Kharif and Rabi separately. If the sum of AUC is lesser than C_{MODIS}, the excess area is added to grasslands. If AUC is greater than C_{MODIS}, the deficit area is subtracted from grasslands, open shrubland and sparsely vegetated regions. This was a needed step to remove inconsistency of data across sources. We have prepared a separate fractional vegetation cover map for Kharif and Rabi seasons each year.

3. Methodology

3.1 VIC Model

VIC model is a semi-distributed macroscale hydrological model that balances water and energy equations grid wise(Liang et al., 1994a). In VIC, within each grid cell, there are tiles based on land use land cover. There is no lateral exchange of fluxes across the grids. While the vegetation properties are different for individual tiles, soil properties do not show any sub-grid variability. Topographic properties can also be represented by incorporating elevation bands within the grid. The final output fluxes are calculated as the area-weighted sum over all the tiles. Users can run the model in two different modes: water balance mode or energy-water balance mode. While in water balance mode, the surface temperature is assumed to be the same as the air temperature, energy balance mode solves for surface temperature iteratively using the energy balance equation.

The input precipitation gets partitioned to ET, change in SM and runoff, in water balance mode. The evaporation from bare soil and canopy evaporation and transpiration from vegetation contribute to the total ET. Potential evaporation occurs when the soil is saturated and is calculated according to the Penman-Montieth equation. Actual evaporation from bare soil is dependent on the SM condition. Based on the water intercepted by the canopy, transpiration and canopy evaporation are calculated. The precipitation reaching the ground infiltrates into the soil and percolates to lower layers. Runoff occurs when the water holding capacity of soil gets exceeded. Baseflow arises from the lowest soil layer in accordance with the Arno formulation. The net radiation is represented as the sum of latent heat flux, sensible heat flux and ground heat flux in the energy balance model (Gao et al., 2010). As a post-processing step, a separate routing model (Lohmann et al., 1996) can be employed to calculate river discharge. Additional features of VIC include snow model(Andreadis et al., 2009), frozen soil algorithm(Cherkauer & Lettenmaier, 1999), lake and wetland model(Bowling & Lettenmaier, 2010), irrigation and reservoir module (I. Haddeland et al., 2006; Ingjerd Haddeland et al., 2006).

VIC version 5 (Hamman et al., 2018), a reconfigured version with improved infrastructure, is used in the present study. It allows parallelization for enhanced computational speed and the option to run space-before-time where all grid cells are processed before proceeding to the next time step. In prior versions, a time-before-space mode was employed where all the time steps for one grid were processed first. The representation of physical processes is similar to previous versions of VIC.

3.2 Irrigation scheme

We have developed and parametrized flood irrigation and drip irrigation schemes to the VIC-5 image driver in the present study. The details regarding the modifications made in the model are described in the following sections.

3.2.1 Flood irrigation

Flood irrigation is the most common mode of irrigation in India, especially in the northwest. It is the least efficient method in terms of field application. In this scheme, water is applied directly to the ground. In the model, we added the irrigation amount($\mathrm{Irr}_{\mathrm{flood}}$) to the precipitation reaching the ground($P^{'}$) mimicking the actual scenario. The net water reaching the ground after irrigation (Q) is hence given by:

$$Q = P^{'} + \mathrm{Irr}_{\mathrm{flood}} \quad (1)$$

As calculated in section 2.2.2, the total irrigation amount is given as an input to the model. It can be either applied daily or intermittently at weekly intervals throughout the irrigation months.

Paddy formulation with flood irrigation

Irrigation practices followed for rice crops are different from other crops. Rice is cultivated in submerged conditions to maximize yield by restricting weed growth. The energy partitioning and water balance mechanisms are different in ponded states. Devanand et al. (2019) added paddy formulations to WRF-CLM4, where water balance modifications were adopted from Xie & Cui (2011), and alterations in surface energy balance were followed according to Masutomi et al. (2016). Here we have elaborated the modifications made for VIC in detail:

a) Water balance

Paddy vegetation bands are differentiated from other bands with a flag. An additional variable is added to represent the depth of ponded water (h) at each time step. h is set to maximum (h_{max}) on the first day of irrigation, as part of field preparation.

When fields are flooded, the bare soil evaporation is replaced with evaporation from open water. Hence, ET is given by:

$$ET = E_{\mathrm{canopy}} + E_{\mathrm{transp.}} + E_{\mathrm{open\ water}} \quad (2)$$

Where, E_{canopy} represents canopy evaporation, $E_{\mathrm{open\ water}}$ is the evaporation from open water and $E_{\mathrm{transp.}}$ is the transpiration.

During land preparation, farmers carry out puddling to ensure the low hydraulic conductivity of the soil. Tilling and compaction fill the soil cracks with smaller particles creating a plow sole with lower permeability (Devanand et al., 2019b; Janssen et al., 2010; Neumann et al., 2009). This ensures the fields remain in a flooded condition. In VIC, the drainage from the first to the second layer is reduced for paddy vegetation bands. This is to account for the plow sole created by the farmers. Due to the presence of ponded water, the topsoil layer is maintained at saturation. The modified drainage (Q_{12})is given by:

$Q_{12} = f_{\text{puddle}} Q_{12,max}$ (3)

Where, $f_{\text{puddle}}$is a fraction between 0 and 1. $Q_{12,max}$ is the drainage from first to second layer when the top soil layer is saturated. We have fixed the value of f_{puddle} as 0.001 as based on the studies by Tsuchiya et al. (2018) and Devanand et al. (2019).

The calculation of runoff is replaced with overbund flow for vegetation bands with paddy. Overbund flow occurs when the depth of ponded water (h) exceeds the bund height (h_{max}). The maximum bund height was fixed to 300mm based on the study conducted in India by Mishra et al. (2008). At a given time step, overbund flow (R_{paddy}) is given by:

$R_{\text{paddy}} = h - h_{\text{max}},\ h > h_{\text{max}}$ (4)

$R_{\text{paddy}} = 0$, h $\leq h_{\text{max}}$ (5)

At the end of each time step, the depth of ponded water (h_{t+1}) is updated on the basis of depth of ponded water at the beginning of the time step (h_t), precipitation reaching the ground ($P^{'}$), irrigation applied (irr), infiltration to the soil (I) and evaporation ($E_{\text{open water}}$). It is given by the following equation:

$h_{t+1} = h_t +\ P^{'} + irr - E_{\text{open water}} - I$ (6)

On the last day of irrigation, the ponded water gets removed as runoff to mimic the practice of farmers' release a few days before harvest.

(b) Energy Balance

The albedo of bare soil is replaced with the albedo of water over the ponded fields. The energy balance equation in VIC is given by:

$R_n = L_g + H + G$ (7)

Where is R$_n$the net radiation, $L_g$is the latent heat flux, H is the sensible heat flux, and G is the ground heat flux. The surface temperature is estimated iteratively according to the following steps (Liang et al., 1994b):

1. At the first time step, the surface temperature is set to the air temperature. Next, the initial values of R$_n$ and ET are determined using this temperature.
2. Equation 7 is iteratively solved for surface temperature.
3. R$_n$ and ET are recalculated using the surface temperature from (b).
4. Final surface temperature for the given time step is estimated by once again solving Equation 7 iteratively.

5. For the next time step, surface temperature from (d) is assumed as the initial temperature, and (b)-(d) are repeated.

For paddy fields, an additional term to incorporate the energy stored is ponded water is added to the energy balance equation. The heat flux stored in the water layer (S_{tw}) is calculated based on the specific heat of water (c_{pw}), the density of water (ρ_w), h and ground temperature (T_g) using the equation (Masutomi et al., 2016):

$$S_{\mathrm{tw}} = c_{\mathrm{pw}} \rho_w h \frac{\partial T_g}{\partial t} \quad (8)$$

The modified energy balance equation is given by:

$$R_n = L_g + H + G + S_{\mathrm{tw}} \quad (9)$$

3.2.2 Drip irrigation

Drip irrigation is the most efficient method of irrigation. The water is applied directly to the root zone based on the SM condition. Here, we perform a check every day at 6 am to find when SM falls below the critical value under which transpiration gets limited. If that is the case, irrigation water($\mathrm{Irr}_{\mathrm{drip}}$) is added to the root zone until the field capacity is reached. The updated soil moisture($\mathrm{SM}^{'}$) is given by:

$$\mathrm{SM}^{'} = SM + \mathrm{Irr}_{\mathrm{drip}} \quad (10)$$

Paddy formulation with drip irrigation

In drip irrigation mode, paddy fields are consistently maintained at saturation during the irrigated months. Therefore, when the SM falls below saturation, irrigation is applied. Like in the flood irrigation formulations, drainage from the first soil layer to the second is less due to the presence of plow sole.

4. Results and Discussions

We performed four sets of simulations in the current study: VIC_CTL, VIC_IRR, VIC_INTER and VIC-DRIP. VIC_CTL represents the model simulation with the default VIC model. Both VIC_IRR and VIC_INTER employ flood irrigation, but the irrigation application is at different frequencies. In the VIC_IRR simulation, irrigation is applied daily at 6 am during the irrigated months. Irrigation application in VIC_INTER is intermittent at weekly intervals. VIC-DRIP represents simulation employing the drip irrigation mode as described in section 3.2.2. All the experiments were performed for a period of 17 years, from 1998 to 2014. For each year, we have used two different fractional vegetation covers for the Kharif and Rabi seasons. We considered a one year of spin-up run to initialize the model. We have presented the results season-wise, i.e., pre-monsoon (MAM), monsoon (JJAS), post-monsoon (ON) and winter (DJF) season.

4.1 Model Performance

We compared the performance of VIC_IRR with VIC_CTL in simulating ET and SM. In Figure 3, the seasonal mean of monthly ET simulated by VIC_CTL and VIC_IRR are compared with GLEAM ET. VIC_IRR outperforms VIC_CTL in capturing the spatial patterns of ET. During the pre-monsoon season, a widespread underestimation of ET can be noted in the VIC_CTL simulation. VIC_IRR simulated ET resembles GLEAM ET over northwest India and the northern stretch of Gangetic plains. The soil remains moist post Rabi irrigation, leading to higher ET during the pre-monsoon season. The grids with high ET over the northern reach indicate irrigation activity. Sugarcane is the predominant crop in this area and is grown around the year. However, over the central and southern stretches of the study region, we find an underestimation in the VIC_IRR simulated ET. It is important to note that we have not considered summer crops in our study, which could be a possible reason for this mismatch. ET simulated in the VIC_IRR experiment exhibits an overestimation during the monsoon season over northwest India and the northern stretch of Gangetic plains. The data corresponding to the interval of irrigation application at different growth stages was not available. Consistent addition of water to the crops in the model on all irrigation days can be attributable to the overestimated ET. The GLEAM derived ET may also have limitations in considering extensive flood irrigation and paddy fields in the main cropping season of India. Hence, there is also a possibility of underestimation of ET by the GLEAM products. During the post-monsoon and winter season, VIC_IRR performs better than VIC_CTL in simulating the spatial patterns in ET, though the magnitudes do not match. Given wetter soil in October subsequent to Kharif irrigation and November marks the beginning of Rabi season, enhanced ET is observed in the VIC_IRR experiment. Since the winter season overlaps with the Rabi season, the VIC_IRR simulated ET is higher than VIC_CTL simulated ET. The western part of Rajasthan is covered with barren land or open shrublands (Figure 2b and 2c) with minimal agricultural activities. Hence, ET over this region is simulated well in both the experiments, during all the seasons.

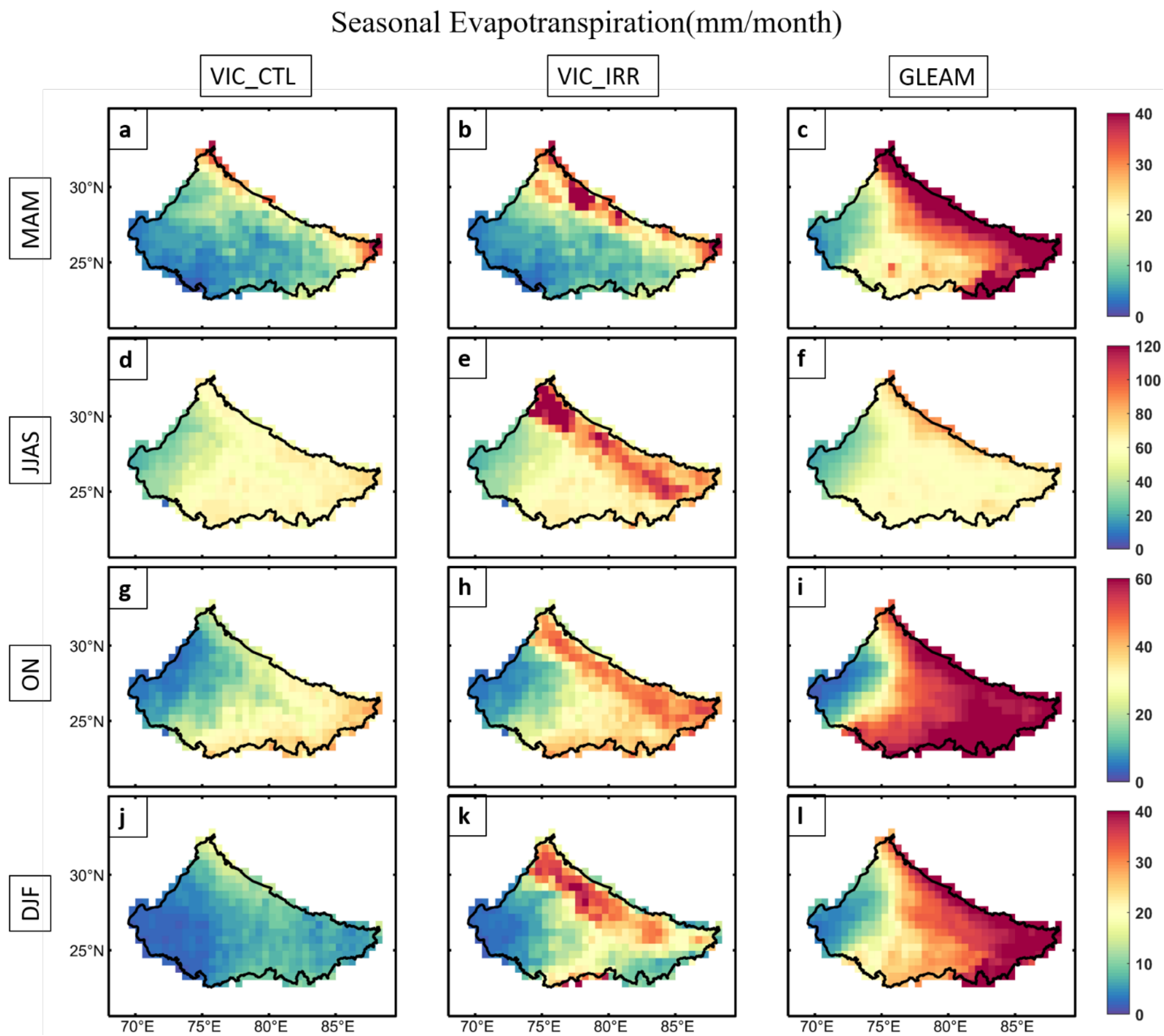

Figure 3. Evaluation of modelled ET against GLEAM ET. Seasonal mean of monthly ET (mm/month) from VIC_CTL (a, d, g, j), VIC_IRR (b, e, h, k) and GLEAM (c, f, i, l) during the period of 1998-2014. Figures (a-c) are for pre-monsoon (MAM), (d-f) for monsoon (JJAS), (g-i) for post-monsoon (ON) and (j-l) for winter (DJF).

We evaluated the seasonal mean of volumetric SM simulated by VIC_CTL and VIC_IRR experiments against ESA CCI SM in Figure 4. The depth covered by satellite observed SM from ESA CCI is 0.5-2cm. Hence, we considered the volumetric SM of the first layer from the model simulations. The simulated and observed SM closely follow the spatial patterns of ET, as expected. During the pre-monsoon season, in the VIC_CTL experiment, we identify a widespread underestimation of volumetric SM. In VIC_IRR simulation, SM over the southern reaches is less than observed due to the non-consideration of summer crops. The grids with sugarcane crops show higher volumetric SM. Similar to the simulated ET during the monsoon season, SM modelled in the VIC_IRR experiment is higher than the ESA CCI SM. However, during the post-monsoon and winter season, VIC_IRR performs well in simulating the spatial pattern of SM. Overall, it is evident that VIC_CTL fails to simulate the irrigation-induced SM during the Rabi season. This limitation is overcome with the VIC_IRR simulations.

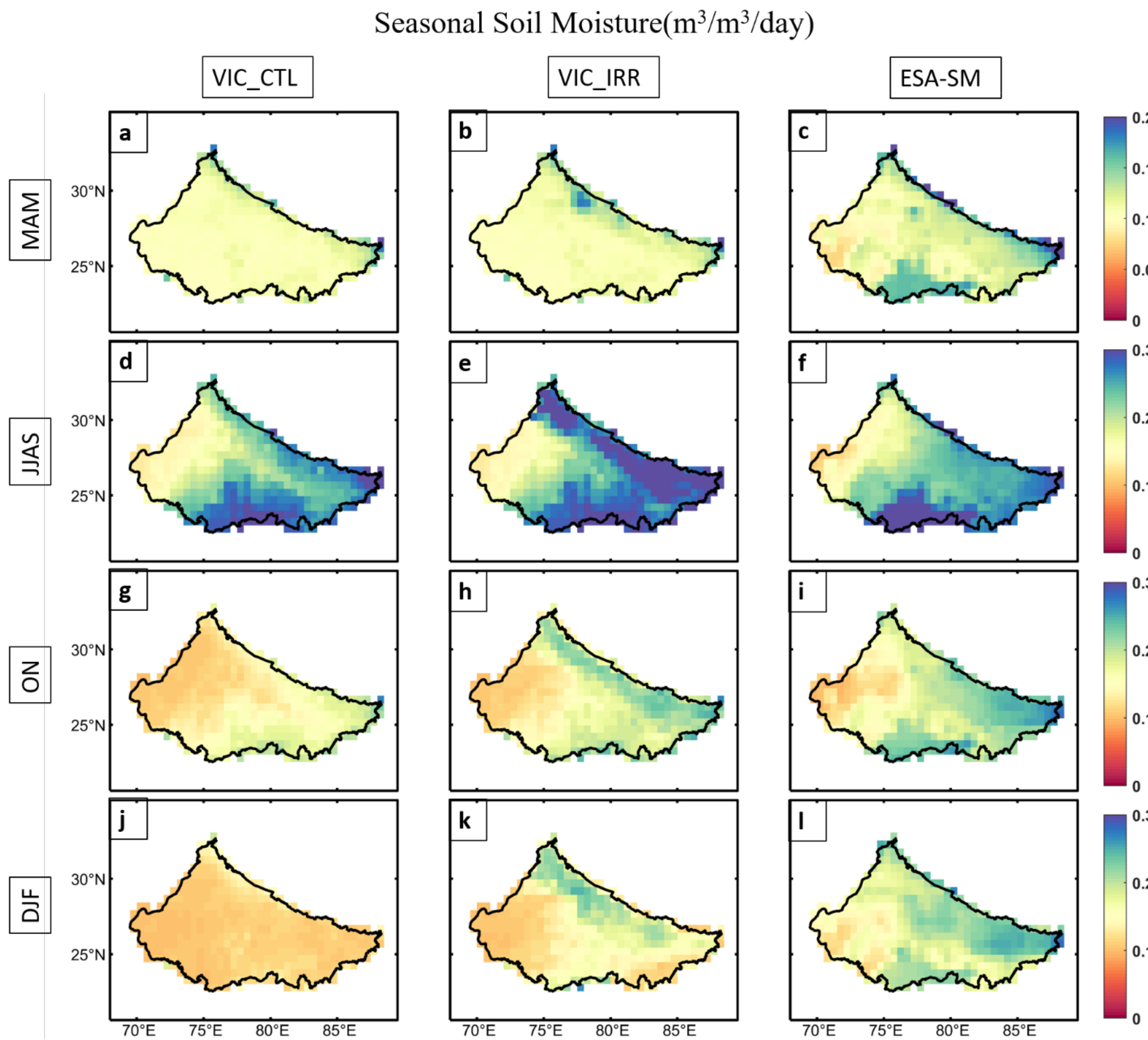

Figure 4. Evaluation of modelled volumetric SM against ESA-SM. Mean seasonal SM (m^3/ m^3/day) from VIC_CTL (a, d, g, j), VIC_IRR (b, e, h, k) and ESA-SM (c, f, i, l) during the period of 1998-2014. Simulated SM of the first layer was considered. Figures (a-c) are for pre-monsoon (MAM), (d-f) for monsoon (JJAS), (g-i) for post-monsoon (ON) and (j-l) for winter (DJF).

4.2 Sensitivity of water fluxes to method of irrigation application

We tested the sensitivity of ET, SM and runoff to the method and frequency of irrigation application. We compared the water fluxes simulated with two different forms of irrigation: demand-driven drip irrigation (VIC_DRIP) and unconstrained flood irrigation (VIC_IRR). In Figure 5, the differences between the seasonal mean of monthly ET simulated by VIC_DRIP and VIC_IRR are depicted. During the pre-monsoon season, no difference was observed in the spatial patterns of VIC_IRR simulated ET and VIC_DRIP simulated ET. The absence of any irrigation activity except over sugarcane dominant grids is a possible reason behind such a result. The major Kharif crop over north-west India is paddy. In the VIC_IRR experiment, bare soil evaporation over ponded paddy fields corresponds to open-water evaporation. Nonetheless, in the VIC_DRIP simulations, since the topsoil layer of paddy fields is maintained at saturation, potential evaporation occurs from bare soil. Consequently, the negative difference between the VIC_DRIP simulated ET and VIC_IRR simulated ET is very high, especially over Punjab and Haryana. Over the Gangetic plains, VIC_DRIP simulated ET is lower than VIC_IRR simulated ET because, in VIC_DRIP, irrigation is based on SM conditions and occurs only when the critical state is reached, unlike VIC_IRR that employs unconstrained flood irrigation. During the post-monsoon season, the differences in ET between the two experiments are less prominent which can be attributed to the absence of irrigation activity during October. The VIC_IRR simulated ET is mildly higher than VIC_DRIP during the Rabi season. This is due to excess water application to the crops in the flood irrigation mode of the VIC_IRR experiment. The unrestrained irrigation in the VIC_IRR simulation can be accounted for the consistent negative difference in ET across all seasons. Conversly, Leng et al. (2014) found ET insensitive to the irrigation technique when the flood irrigation is demand-driven.

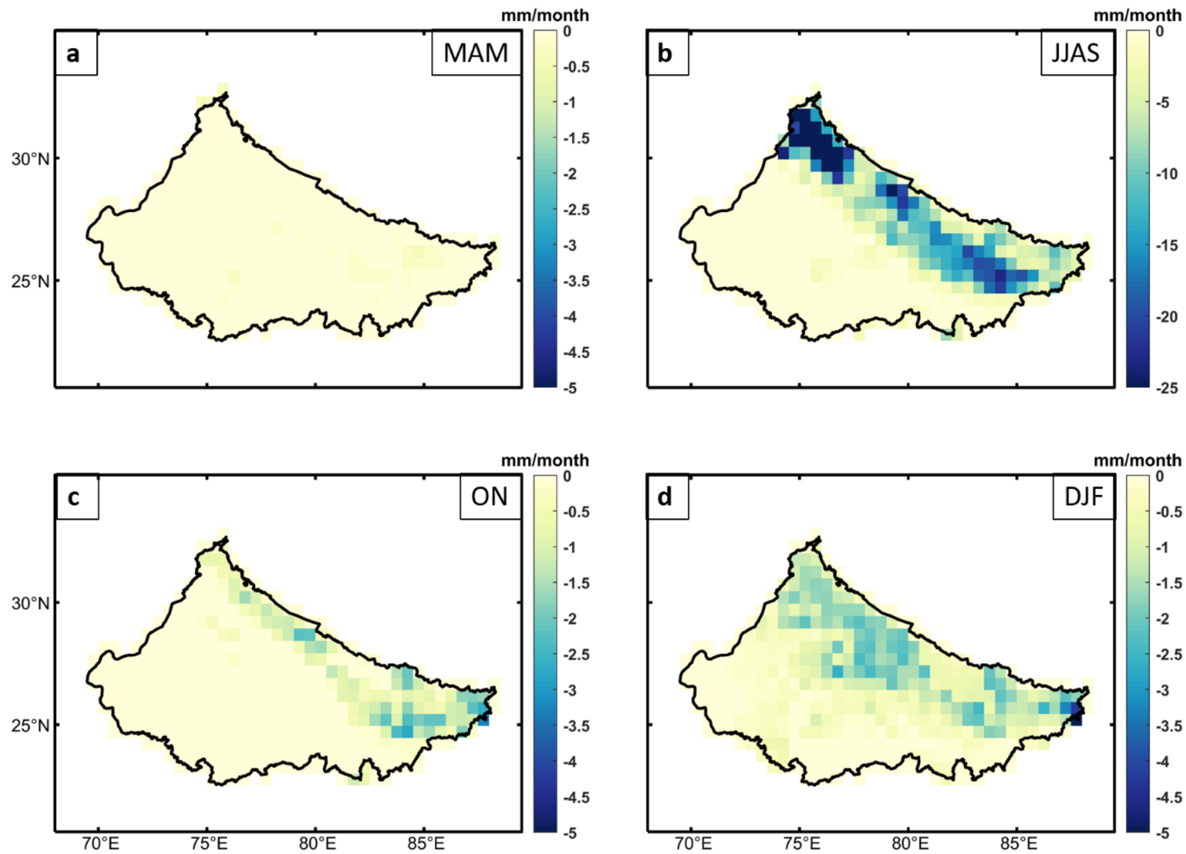

Figure 5. Differences between the seasonal mean of monthly ET simulated by VIC_DRIP and VIC_IRR during (a) pre-monsoon, (b) monsoon (c) post-monsoon and (d) winter.

Figure 6 shows the differences between the seasonal mean of volumetric surface SM simulated by VIC_DRIP and VIC_IRR. During the pre-monsoon season, zero differences indicate that the spatial patterns of SM simulated from VIC_DRIP and VIC_IRR match precisely. We noted mild negative differences over northwestern India and the Gangetic plains during the monsoon season. The SM over paddy fields in both experiments is maintained at saturation. Hence, the differences in SM are less pronounced when compared to the differences in ET during the Kharif season. The SM simulated by VIC_DRIP is slightly lower than the VIC_FLOOD simulated ET during the post-monsoon season analogous to ET in Figure 5. As expected, there is a considerable negative difference during the winter season, indicating higher SM in VIC_IRR simulation. The differences between the seasonal mean of daily runoff simulated by VIC_DRIP and VIC_IRR are demonstrated in Figure 7. During the pre-monsoon season, the VIC_IRR simulated runoff is higher over the sugarcane cultivated grids. The differences in runoff are maximum during the monsoon season, followed by the winter season. Consistent negative differences across all the seasons are due to the surplus water application in flood irrigation mode of the VIC_IRR experiment.

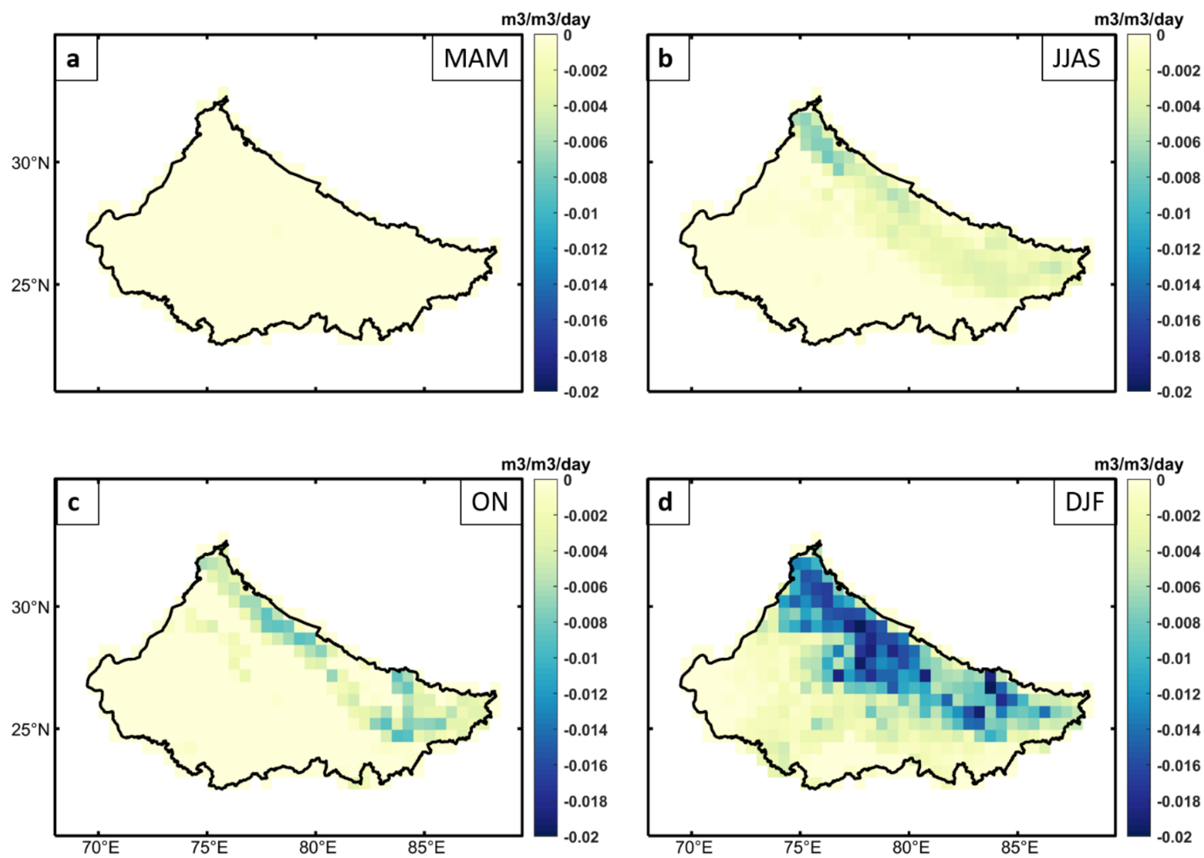

Figure 6. Differences between the seasonal mean of volumetric SM simulated by VIC_DRIP and VIC_IRR during (a) pre-monsoon, (b) monsoon (c) post-monsoon and (d) winter.

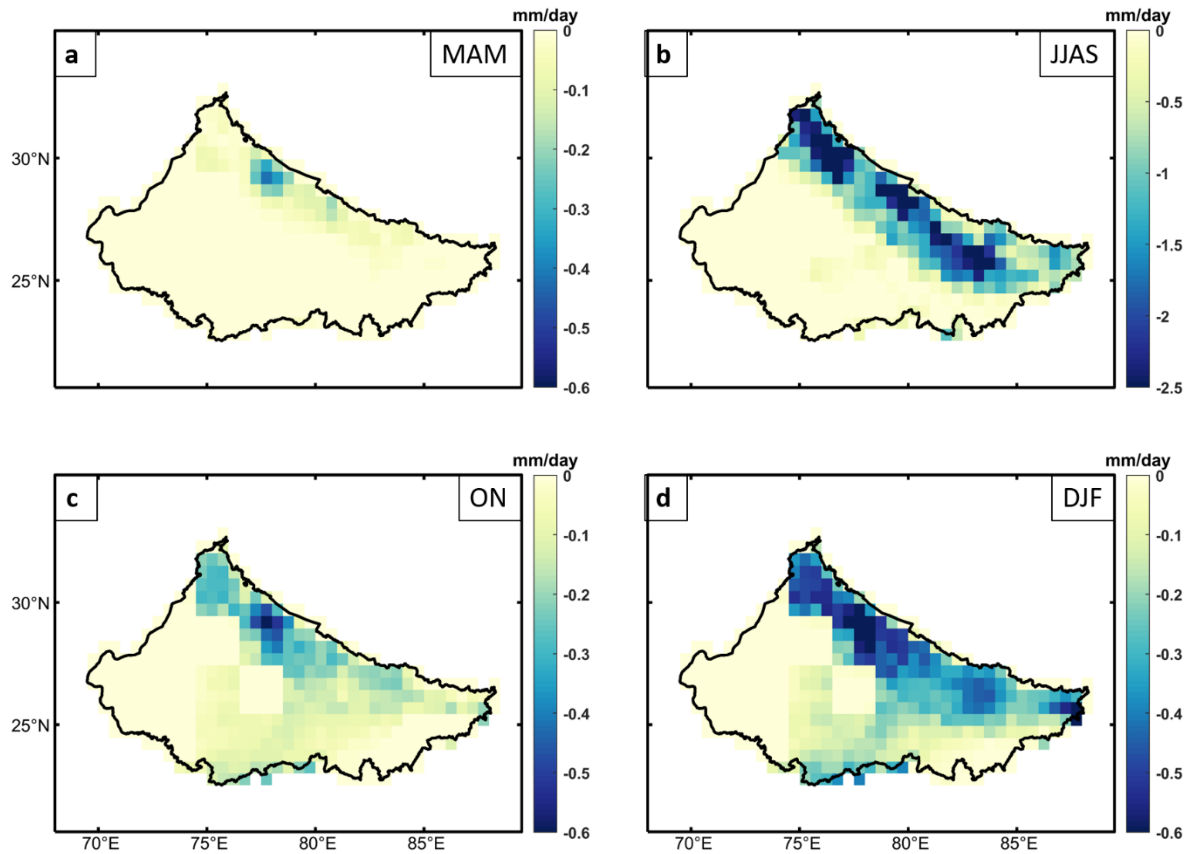

Figure 7. Differences between the seasonal mean of runoff simulated by VIC_DRIP and VIC_IRR during (a) pre-monsoon, (b) monsoon (c) post-monsoon and (d) winter

We also tested the sensitivity of the simulations to the frequency of irrigation applications. We performed the VIC_INTER experiment by applying irrigation water once every 7days. The only change from VIC_IRR is the frequency at which water is added to the crop fields with same total seasonal irrigation applications. The ET simulated by VIC_INTER is slightly lower than VIC_IRR simulated ET over a few grids during the pre-monsoon and monsoon season (Supplementary Figure S1). Limited moisture availability between two consecutive irrigation applications could be a possible reason for lower ET in VIC_INTER. The differences in ET are less prominent during the other seasons. SM shows insignificant sensitivity to the interval of irrigation application (Supplementary FigureS2). In Figure 8, we have plotted the difference between VIC_INTER simulated runoff and VIC_IRR simulated runoff. In general, the runoff estimated in the VIC_INTER experiment is higher than VIC_IRR across all seasons. The difference is subtle during the pre-monsoon and winter seasons. In the VIC_INTER experiment, water is applied all at once at the beginning of every week, resulting in a higher runoff. The differences in runoff are more noticeable during the monsoon and post-monsoon seasons. The antecedent moist soil due to precipitation leads to excess runoff during these seasons. We compared the time series of ET, SM and runoff spatially averaged over irrigated grids generated from VIC_IRR, VIC_DRIP and VIC_INTER (Supplementary Figure S3). The time series of VIC_IRR and VIC_INTER estimated ET are identical and exceed VIC_DRIP simulated ET during the monsoon season. Runoff is highly sensitive, whereas SM is least susceptible to the technique and frequency of irrigation.

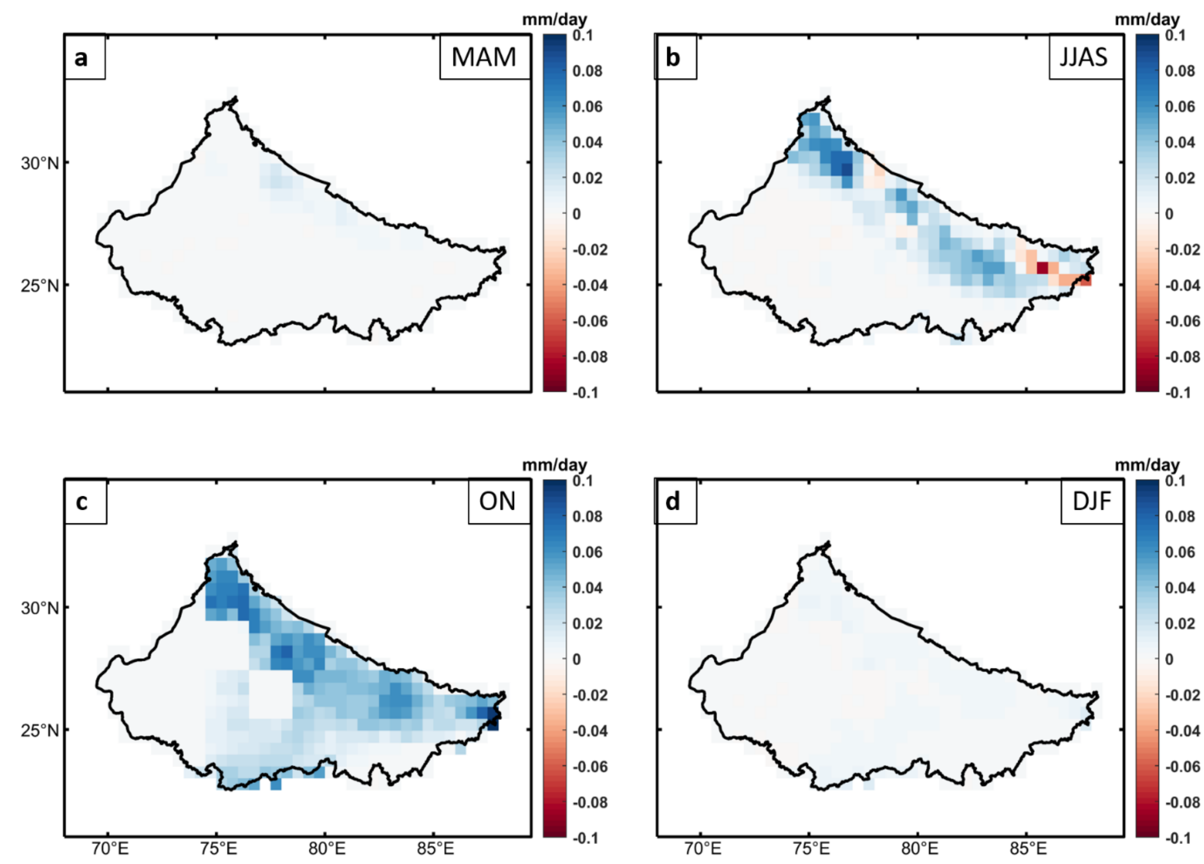

Figure 8. Differences between the seasonal mean of runoff simulated by VIC_INTER and VIC_IRR during (a) pre-monsoon, (b) monsoon (c) post-monsoon and (d) winter

5. Conclusion

Our study developed a new irrigation scheme designed to suit Indian agricultural practices for widely used VIC. The irrigation water is supplied as an input to the model, in contrast to the parametrization in conventional irrigation coupled hydrological models. The water cycle and energy partitioning of paddy fields under submerged conditions are formulated separately. We have also tested the sensitivity of ET, SM and runoff to the frequency and technique of irrigation application. The major conclusions of our study are:

1. VIC_IRR performs better than VIC_CTL in replicating the observed spatial patterns of ET and SM, specifically during the non-monsoon seasons. However, during the monsoon season, VIC_IRR overestimates ET and SM.

2. We noted a strong response of ET on the technique of irrigation employed, particularly during the monsoon season. The ET estimated in the VIC_DRIP experiment is lower than VIC_IRR simulated ET due to judicious irrigation application in the former. ET is less sensitive to the interval at which irrigation is applied to the fields.

3. SM responded significantly to the irrigation methods during the relatively drier Rabi season. Minimal differences between VIC_DRIP and VIC_IRR simulated SM were noted during other seasons. The frequency of irrigation application has a negligible effect on SM across all seasons.

4. The difference between the VIC_DRIP and VIC_IRR simulated runoff is more prominent during the irrigated months indicating its high sensitivity to the irrigation technique. Runoff is also influenced by the interval of irrigation application, mainly in the wetter months.

Here, we attempt to address the limitations in traditional irrigation-coupled hydrological models through the newly proposed irrigation scheme. A previous study over India using the VIC irrigation module suggested an over-estimation of agricultural water use even though it employed demand-driven sprinkler irrigation (Shah et al.,2019). The apparent limitation of this study was the non-consideration of groundwater as a source of irrigation. Conversely, we find that the actual irrigation water use is way higher than that estimated based on SM conditions. Another clear advantage of our model is the separate formulation of submerged paddy fields. We also observe that the water fluxes are sensitive to the method and interval of irrigation application. Therefore, we like to draw attention to the fact that there are significant biases in the previously estimated irrigation-induced effects on the water cycle. We highlight the importance of the precise representation of irrigation practices in impact studies to plan for appropriate adaptation strategies.

Our study has certain limitations. Though water use data are recorded based on field experience, it may vary according to farmer behaviour (O'Keeffe et al., 2018). In terms of quantity and frequency, the irrigation application depends on the stage of plant development and growth. Data pertaining to irrigation scheduling is limited. The district-wise area under each crop and the irrigated fraction is assumed to be uniformly distributed over the region. Thus, there exists an ambiguity in the exact location of individual crop fields, though negligible in macroscale hydrological modelling. Here, we have not taken into account the source of irrigation water since it requires interaction with groundwater and surface water. The future scope of this study will be to analyze the effects of unrestrained irrigation on the depth of groundwater and its dependence on the choice of irrigation methods.

Acknowledgments

The work is financially supported by Department of Science and Technology Swarnajayanti Fellowship Scheme, through project no. DST/ SJF/ E&ASA-01/2018-19; SB/SJF/2019-20/11. The work was initiated through a funding support from Ministry of Earth Sciences, Government of India, and National Environment Research Council (NERC), UK through project no. MOES/NERC/IA-SWR/P2/09/2016-PC-II. The authors thank Prof. P P Mujumdar for providing useful suggestions related to this work. All the data used in this work are online available and the sources are mentioned in the text.

References

Alcamo, J., Döll, P., Henrichs, T., Kaspar, F., Lehner, B., Rösch, T., & Siebert, S. (2003). Development and testing of the WaterGAP 2 global model of water use and availability. *Hydrological Sciences Journal*, *48*(3), 317–337. https://doi.org/10.1623/hysj.48.3.317.45290

Andreadis, K. M., Storck, P., & Lettenmaier, D. P. (2009). Modeling snow accumulation and ablation processes in forested environments. *Water Resources Research*, *45*(5), 1–13. https://doi.org/10.1029/2008WR007042

Asoka, A., Gleeson, T., Wada, Y., & Mishra, V. (2017). Relative contribution of monsoon precipitation and pumping to changes in groundwater storage in India. *Nature Geoscience*, *10*(2), 109–117. https://doi.org/10.1038/ngeo2869

Balakrishnan, K., Natarajaratnam, N., & Rajendran, C. (1987). Critical Leaf Area Index in Pigeonpea. *Journal of Agronomy and Crop Science*, *159*(3), 164–166. https://doi.org/10.1111/j.1439-037X.1987.tb00081.x

Bandyopadhyay, K. K., Misra, A. K., Ghosh, P. K., & Hati, K. M. (2010). Effect of integrated use of farmyard manure and chemical fertilizers on soil physical properties and productivity of soybean. *Soil and Tillage Research*, *110*(1), 115–125. https://doi.org/10.1016/j.still.2010.07.007

Barik, B., Ghosh, S., Saheer Sahana, A., Pathak, A., & Sekhar, M. (2017). Water-food-energy nexus with changing agricultural scenarios in India during recent decades. *Hydrology and Earth System Sciences*, *21*(6), 3041–3060. https://doi.org/10.5194/hess-21-3041-2017

Bohn, T. J., Livneh, B., Oyler, J. W., Running, S. W., Nijssen, B., & Lettenmaier, D. P. (2013). Global evaluation of MTCLIM and related algorithms for forcing of ecological and hydrological models. *Agricultural and Forest Meteorology*, *176*, 38–49. https://doi.org/10.1016/j.agrformet.2013.03.003

Boken, V. K., & Chandra, S. (2012). Estimating Leaf Area Index for an arid region using Spectral Data. *African Crop Science Journal*, *20*(4), 215–224.

Bowling, L. C., & Lettenmaier, D. P. (2010). Modeling the Effects of Lakes and Wetlands on the Water Balance of Arctic Environments. *Journal of Hydrometeorology*, *11*(2), 276–295. https://doi.org/10.1175/2009JHM1084.1

Bsaibes, A., Courault, D., Baret, F., Weiss, M., Olioso, A., Jacob, F., et al. (2009). Albedo and LAI estimates from FORMOSAT-2 data for crop monitoring. *Remote Sensing of Environment*, *113*(4), 716–729. https://doi.org/10.1016/j.rse.2008.11.014

Chandel, V. S., & Ghosh, S. (2021). Components of Himalayan River Flows in a Changing Climate. *Water Resources Research*, *57*(2). https://doi.org/10.1029/2020WR027589

Chawla, I., & Mujumdar, P. P. (2015). Isolating the impacts of land use and climate change on streamflow. *Hydrology and Earth System Sciences*, *19*(8), 3633–3651. https://doi.org/10.5194/hess-19-3633-2015

Chen, Y., Niu, J., Kang, S., & Zhang, X. (2018). Effects of irrigation on water and energy balances in the Heihe River basin using VIC model under different irrigation scenarios. *Science of the Total Environment*, *645*, 1183–1193. https://doi.org/10.1016/j.scitotenv.2018.07.254

Cherkauer, K. A., & Lettenmaier, D. P. (1999). Hydrologic effects of frozen soils in the upper Mississippi River basin, *104(D16)*, 19599–19610.

Chou, C., Ryu, D., Lo, M. H., Wey, H. W., & Malano, H. M. (2018). Irrigation-induced land-atmosphere feedbacks and their impacts on Indian summer monsoon. *Journal of Climate*, *31*(21), 8785–8801. https://doi.org/10.1175/JCLI-D-17-0762.1

Davis, K. F., Chiarelli, D. D., Rulli, M. C., Chhatre, A., Richter, B., Singh, D., & DeFries, R. (2018). Alternative cereals can improve water use and nutrient supply in India. *Science Advances*, *4*(7), 1–11. https://doi.org/10.1126/sciadv.aao1108

Devanand, A., Huang, M., Ashfaq, M., Barik, B., & Ghosh, S. (2019). Choice of Irrigation Water Management Practice Affects Indian Summer Monsoon Rainfall and Its Extremes Geophysical Research Letters, 9126–9135. https://doi.org/10.1029/2019GL083875

Devineni, N., Perveen, S., & Lall, U. (2013). Assessing chronic and climate-induced water risk through spatially distributed cumulative deficit measures: A new picture of water sustainability in India. *Water Resources Research*, *49*(4), 2135–2145. https://doi.org/10.1002/wrcr.20184

Directorate of Economics Statistics. (2018). Agriculture statistics at a glance. *Goi*, 1–502.

Döll, P. (2002). Impact of climate change and variability on irrigation requirements: A global perspective. *Climatic Change*, *54*(3), 269–293. https://doi.org/10.1023/A:1016124032231

Döll, P., Kaspar, F., & Lehner, B. (2003). A global hydrological model for deriving water availability indicators: Model tuning and validation. *Journal of Hydrology*, *270*(1–2), 105–134. https://doi.org/10.1016/S0022-1694(02)00283-4

Douglas, E. M., Beltrán-Przekurat, A., Niyogi, D., Pielke, R. A., & Vörösmarty, C. J. (2009). The impact of agricultural intensification and irrigation on land-atmosphere interactions and Indian monsoon precipitation - A mesoscale modeling perspective. *Global and Planetary Change*, *67*(1–2), 117–128. https://doi.org/10.1016/j.gloplacha.2008.12.007

Douglas, Ellen M., Niyogi, D., Frolking, S., Yeluripati, J. B., Pielke, R. A., Niyogi, N., et al. (2006). Changes in moisture and energy fluxes due to agricultural land use and irrigation in the Indian Monsoon Belt. *Geophysical Research Letters*, *33*(14), 1–5. https://doi.org/10.1029/2006GL026550

Droppers, B., Franssen, W. H. P., Van Vliet, M. T. H., Nijssen, B., & Ludwig, F. (2020). Simulating human impacts on global water resources using VIC-5. *Geoscientific Model Development*, *13*(10), 5029–5052. https://doi.org/10.5194/gmd-13-5029-2020

Fan, J., McConkey, B., Wang, H., & Janzen, H. (2016). Root distribution by depth for temperate agricultural crops. *Field Crops Research*, *189*, 68–74. https://doi.org/10.1016/j.fcr.2016.02.013

Fishman, R., Devineni, N., & Raman, S. (2015). Can improved agricultural water use efficiency save India's groundwater? *Environmental Research Letters*, *10*(8), 84022. https://doi.org/10.1088/1748-9326/10/8/084022

Foley, J. A., DeFries, R., Asner, G. P., Barford, C., Bonan, G., Carpenter, S. R., et al. (2005). Global consequences of land use. *Science*, *309*(5734), 570–574. https://doi.org/10.1126/science.1111772

Foley, J. A., Ramankutty, N., Brauman, K. A., Cassidy, E. S., Gerber, J. S., Johnston, M., et al. (2011). Solutions for a cultivated planet. *Nature*, *478*(7369), 337–342. https://doi.org/10.1038/nature10452

Food, W. (2020). *World Food and Agriculture - Statistical Yearbook 2020. World Food and Agriculture - Statistical Yearbook 2020.* https://doi.org/10.4060/cb1329en

Gadi, V. K., Bordoloi, S., Garg, A., Kobayashi, Y., & Sahoo, L. (2016). Improving and correcting unsaturated soil hydraulic properties with plant parameters for agriculture and bioengineered slopes. *Rhizosphere*, *1*(October), 58–78. https://doi.org/10.1016/j.rhisph.2016.07.003

Gao, H., Tang, Q., Shi, X., Zhu, C., & Bohn, T. (2010). Water budget record from Variable Infiltration Capacity (VIC) model. *Algorithm Theoretical Basis Document for Terrestrial Water Cycle Data Records*, (Vic), 120–173. Retrieved from http://scholar.google.com/scholar?hl=en&btnG=Search&q=intitle:Water+Budget+Record+from+Varia

Garg, R. N., Gupta, V. K., Singh, S., Tomar, R. K., & Chakraborty, D. (2014). Growth Assessment of Wheat using Remote Sensing Techniques under Various Mulch and Nitrogen Levels in a Semi-arid Delhi Region. *Journal of Agricultural Physics*, *14*(1), 44–49.

Ghosh, S., Vittal, H., Sharma, T., Karmakar, S., Kasiviswanathan, K. S., Dhanesh, Y., et al. (2016). Indian Summer Monsoon Rainfall: Implications of Contrasting Trends in the Spatial Variability of Means and Extremes. *PloS One*, *11*(7), e0158670. https://doi.org/10.1371/journal.pone.0158670

Ghule, P. L., Jadhav, J. D., Palve, D. K., & Dahiphale, V. V. (2013). Bt cotton and its leaf area index (LAI), ginning (%), lint index (g), earliness index and yield contributing characters, *4*(1), 85–90.

Godfray, H. C. J., Beddington, J. R., Crute, I. R., Haddad, L., Lawrence, D., Muir, J. F., et al. (2010). Food Security: The Challenge of Feeding 9 Billion People. *Science*, *327*(5967), 812–818. https://doi.org/10.1126/SCIENCE.1185383

Gomathi, R., Rao, P. N. G., Rakkiyappan, P., Sundara, B. P., & Shiyamala, S. (2013). Physiological Studies on Ratoonability of Sugarcane Varieties under Tropical Indian Condition. *American Journal of Plant Sciences*, *04*(02), 274–281. https://doi.org/10.4236/ajps.2013.42036

Guimberteau, M., Laval, K., Perrier, A., & Polcher, J. (2012). Global effect of irrigation and its impact on the onset of the Indian summer monsoon. *Climate Dynamics*, *39*(6), 1329–1348. https://doi.org/10.1007/s00382-011-1252-5

Haddeland, I., Skaugen, T., & Lettenmaier, D. P. (2006). Hydrologic effects of land and water management in North America and Asia: 1700–1992. *Hydrology and Earth System Sciences Discussions*, *3*(5), 2899–2922. https://doi.org/10.5194/hessd-3-2899-2006

Haddeland, Ingjerd, Lettenmaier, D. P., & Skaugen, T. (2006). Effects of irrigation on the water and energy balances of the Colorado and Mekong river basins. *Journal of Hydrology*, *324*(1–4), 210–223. https://doi.org/10.1016/j.jhydrol.2005.09.028

Haddeland, Ingjerd, Heinke, J., Biemans, H., Eisner, S., Flörke, M., Hanasaki, N., et al. (2014). Global water resources affected by human interventions and climate change. *Proceedings of the National Academy of Sciences of the United States of America*, *111*(9), 3251–3256. https://doi.org/10.1073/pnas.1222475110

Hamman, J. J., Nijssen, B., Bohn, T. J., Gergel, D. R., & Mao, Y. (2018). The Variable Infiltration Capacity Model, Version 5 (VIC-5): Infrastructure improvements for new applications and reproducibility. *Geoscientific Model Development*, *5*(March), 3481–3496. https://doi.org/10.5194/gmd-11-3481-2018

Hanasaki, N., Kanae, S., Oki, T., Masuda, K., Motoya, K., Shirakawa, N., et al. (2008a). An integrated model for the assessment of global water resources - Part 1: Model description and input meteorological forcing. *Hydrology and Earth System Sciences*, *12*(4), 1007–1025. https://doi.org/10.5194/hess-12-1007-2008

Hanasaki, N., Kanae, S., Oki, T., Masuda, K., Motoya, K., Shirakawa, N., et al. (2008b). An integrated model for the assessment of global water resources - Part 2: Applications and assessments. *Hydrology and Earth System Sciences*, *12*(4), 1027–1037. https://doi.org/10.5194/hess-12-1027-2008

Janssen, M., Lennartz, B., & Wöhling, T. (2010). Percolation losses in paddy fields with a dynamic soil structure: Model development and applications. *Hydrological Processes*, *24*(7), 813–824. https://doi.org/10.1002/hyp.7525

Jaramillo, F., & Destouni, G. (2015). Local flow regulation and irrigation raise global human water consumption and footprint. *Science (New York, N.Y.)*, *350*(6265), 1248–51. https://doi.org/10.1126/science.aad1010

Konlan, S., J, S.-A., E, A., H, A.-D., & MJ., K. (2013). Groundnut(Arachis hypogaea L.) varietal response to spacing in the humid forest zone of Ghana. *ARPN Journal of Agricultural and Biological Science*, *8*(9), 642–651. Retrieved from www.arpnjournals.com

Kour, R., Sharma, B. C., Kumar, A., Kour, P., & Nandan, B. (2016). Study of physiological growth indices of chickpea in chickpea (Cicer arietinum) + mustard (Brassica juncea) intercropping system under different weed management practices. *Legume Research*, *39*(3), 453–458. https://doi.org/10.18805/lr.v0iOF.9439

Kueppers, L. M., & Snyder, M. A. (2012). Influence of irrigated agriculture on diurnal surface energy and water fluxes, surface climate, and atmospheric circulation in California. *Climate Dynamics*, *38*(5–6), 1017–1029. https://doi.org/10.1007/s00382-011-1123-0

Lal, M. (2011). Implications of climate change in sustained agricultural productivity in South Asia. *Regional Environmental Change*, *11*(SUPPL. 1), 79–94. https://doi.org/10.1007/s10113-010-0166-9

Leng, G., Huang, M., Tang, Q., Gao, H., & Leung, L. R. (2014). Modeling the Effects of Groundwater-Fed Irrigation on Terrestrial Hydrology over the Conterminous United States. *Journal of Hydrometeorology*, *15*(3), 957–972. https://doi.org/10.1175/JHM-D-13-049.1

Leng, G., Leung, L. R., & Huang, M. (2014). Significant impacts of irrigation water sources and methods on modeling irrigation effects in the ACME Land Model. *Journal of Advances in Modeling Earth Systems*, *6*, 513–526. https://doi.org/10.1002/2013MS000282.Received

Leng, G., Tang, Q., Huang, M., & Leung, L. (2015a). A comparative analysis of the impacts of climate change and irrigation on land surface and subsurface hydrology in the North China Plain. *Regional Environmental Change*, *15*(2), 251–263. https://doi.org/10.1007/s10113-014-0640-x

Leng, G., Tang, Q., Huang, M., & Leung, L. (2015b). A comparative analysis of the impacts of climate change and irrigation on land surface and subsurface hydrology in the North China Plain. *Regional Environmental Change*, *15*(2), 251–263. https://doi.org/10.1007/s10113-014-0640-x

Li, X., & Troy, T. J. (2018). Changes in rainfed and irrigated crop yield response to climate in the western US. *Environmental Research Letters*, *13*(6). https://doi.org/10.1088/1748-9326/aac4b1

Liang, X., Lettenmaier, D. P., Wood, E. F., & Burges, S. J. (1994a). A simple hydrologically based model of land surface water and energy fluxes for general circulation models. *Journal of Geophysical Research*, *99*(D7), 14415. https://doi.org/10.1029/94JD00483

Liang, X., Lettenmaier, D. P., Wood, E. F., & Burges, S. J. (1994b). A simple hydrologically based model of land surface water and energy fluxes for general circulation models. *Journal of Geophysical Research: Atmospheres*, *99*(D7), 14415–14428. https://doi.org/10.1029/94JD00483

Lo, M. H., & Famiglietti, J. S. (2013). Irrigation in California's Central Valley strengthens the southwestern U.S. water cycle. *Geophysical Research Letters*, *40*(2), 301–306. https://doi.org/10.1002/grl.50108

Lohmann, D., NolteHolube, R., & Raschke, E. (1996). A large-scale horizontal routing model to be coupled to land surface parametrization schemes. *Tellus Series A-Dynamic Meteorology and Oceanography*. https://doi.org/10.1034/j.1600-0870.1996.t01-3-00009.x

Malek, K., Stöckle, C., Chinnayakanahalli, K., Nelson, R., Liu, M., Rajagopalan, K., et al. (2017). VIC-CropSyst-v2: A regional-scale modeling platform to simulate the nexus of climate, hydrology, cropping systems, and human decisions. *Geoscientific Model Development*, *10*(8), 3059–3084. https://doi.org/10.5194/gmd-10-3059-2017

Martens, B., Miralles, D. G., Lievens, H., Van Der Schalie, R., De Jeu, R. A. M., Fernández-Prieto, D., et al. (2017). GLEAM v3: Satellite-based land evaporation and root-zone soil moisture. *Geoscientific Model Development*, *10*(5), 1903–1925. https://doi.org/10.5194/gmd-10-1903-2017

Masutomi, Y., Ono, K., Mano, M., Maruyama, A., & Miyata, A. (2016). A land surface model combined with a crop growth model for paddy rice (MATCRO-Rice v. 1) - Part 1: Model description. *Geoscientific Model Development*, *9*(11), 4133–4154. https://doi.org/10.5194/gmd-9-4133-2016

Mishra, S. K., Sarkar, R., Dutta, S., & Panigrahy, S. (2008). A physically based hydrological model for paddy agriculture dominated hilly watersheds in tropical region. *Journal of Hydrology*, *357*(3–4), 389–404. https://doi.org/10.1016/j.jhydrol.2008.05.019

Mishra, V., Ambika, A. K., Asoka, A., Aadhar, S., Buzan, J., Kumar, R., & Huber, M. (2020). Moist heat stress extremes in India enhanced by irrigation. *Nature Geoscience*, *13*(11), 722–728. https://doi.org/10.1038/s41561-020-00650-8

Neumann, R. B., Polizzotto, M. L., Badruzzaman, A. B. M., Ali, M. A., Zhang, Z., & Harvey, C. F. (2009). Hydrology of a groundwater-irrigated rice field in Bangladesh: Seasonal and daily mechanisms of infiltration. *Water Resources Research*, *45*(9), 1–14. https://doi.org/10.1029/2008WR007542

Nijssen, B., Schnur, R., & Lettenmaier, D. P. (2001). Global retrospective estimation of soil moisture using the variable infiltration capacity land surface modl, 1980-93. *Journal of Climate*, *14*(8), 1790–1808. https://doi.org/10.1175/1520-0442(2001)014<1790:GREOSM>2.0.CO;2

Nijssen, Bart, O'Donnell, G. M., Lettenmaier, D. P., Lohmann, D., & Wood, E. F. (2001). Predicting the discharge of global rivers. *Journal of Climate*, *14*(15), 3307–3323. https://doi.org/10.1175/1520-0442(2001)014<3307:PTDOGR>2.0.CO;2

Niroula, S., Halder, S., & Ghosh, S. (2018). Perturbations in the initial soil moisture conditions: Impacts on hydrologic simulation in a large river basin. *Journal of Hydrology*, *561*(April), 509–522. https://doi.org/10.1016/j.jhydrol.2018.04.029

Niyogi, D., Kishtawal, C., Tripathi, S., & Govindaraju, R. S. (2010). Observational evidence that agricultural intensification and land use change may be reducing the Indian summer monsoon rainfall. *Water Resources Research*, *46*(3), 1–17. https://doi.org/10.1029/2008WR007082

O'Keeffe, J., Moulds, S., Bergin, E., Brozović, N., Mijic, A., & Buytaert, W. (2018). Including Farmer Irrigation Behavior in a Sociohydrological Modeling Framework With Application in North India. *Water Resources Research*, 4849–4866. https://doi.org/10.1029/2018WR023038

Pokhrel, Y., Hanasaki, N., Koirala, S., Cho, J., Yeh, P. J. F., Kim, H., et al. (2012). Incorporating anthropogenic water regulation modules into a land surface model. *Journal of Hydrometeorology*, *13*(1), 255–269. https://doi.org/10.1175/JHM-D-11-013.1

Portmann, F. T., Siebert, S., & Döll, P. (2010). MIRCA2000-Global monthly irrigated and rainfed crop areas around the year 2000: A new high-resolution data set for agricultural and hydrological modeling. *Global Biogeochemical Cycles*, *24*(1), n/a-n/a. https://doi.org/10.1029/2008gb003435

Puma, M. J., & Cook, B. I. (2010). Effects of irrigation on global climate during the 20th century. *Journal of Geophysical Research Atmospheres*, *115*(16), 1–15. https://doi.org/10.1029/2010JD014122

Rajagopalan, K., Chinnayakanahalli, K. J., Stockle, C. O., Nelson, R. L., Kruger, C. E., Brady, M. P., et al. (2018). Impacts of Near-

Term Climate Change on Irrigation Demands and Crop Yields in the Columbia River Basin. *Water Resources Research*, *54*(3), 2152–2182. https://doi.org/10.1002/2017WR020954

Raje, D., Priya, P., & Krishnan, R. (2014). Macroscale hydrological modelling approach for study of large scale hydrologic impacts under climate change in Indian river basins. *Hydrological Processes*, *28*(4), 1874–1889. https://doi.org/10.1002/hyp.9731

Rajeevan, M., & Bhate, J. (2009). A high resolution gridded rainfall dataset (1971-2005) for mesoscale meteorological studies. *Current Science*, *96*(4), 558–562.

Rajeevan, M., Bhate, J., Kale, J. D., & Lal, B. (2006). High resolution daily gridded rainfall data for the Indian region: Analysis of break and active monsoon spells. *Current Science*, *91*(3), 296–306.

Rao, N. R., Garg, P. K., Ghosh, S. K., & Section, G. E. (2006). Estimation and comparison of leaf area index of agricultural crops using IRS LISS-III and EO-1 hyperion images, *34*(I).

Reddy, M. S., & Willey, R. W. (1981). Growth and resource use studies in an intercrop of pearl millet/groundnut. *Field Crops Research*, *4*(C), 13–24. https://doi.org/10.1016/0378-4290(81)90050-2

Rockström, J., Steffen, W., K. Noone, Å. Persson, F. S. Chapin, E. F. Lambin, et al. (2009). A safe operation space for humanity. *Nature*, *461*(September), 472–475.

de Rosnay, P., Polcher, J., Laval, K., & Sabre, M. (2003). Integrated parameterization of irrigation in the land surface model ORCHIDEE. Validation over Indian Peninsula. *Geophysical Research Letters*, *30*(19), 1–4. https://doi.org/10.1029/2003GL018024

Saeed, F., Hagemann, S., & Jacob, D. (2009). Impact of irrigation on the South Asian summer monsoon. *Geophysical Research Letters*, *36*(20), 1–7. https://doi.org/10.1029/2009GL040625

Saha, A., Joseph, J., & Ghosh, S. (2020). Climate controls on the terrestrial water balance: Influence of aridity on the basin characteristics parameter in the Budyko framework. *Science of the Total Environment*, *739*, 139863. https://doi.org/10.1016/j.scitotenv.2020.139863

Shah, H. L., Zhou, T., Sun, N., Huang, M., & Mishra, V. (2019). Roles of Irrigation and Reservoir Operations in Modulating Terrestrial Water and Energy Budgets in the Indian Subcontinental River Basins. *Journal of Geophysical Research: Atmospheres*, *124*(23), 12915–12936. https://doi.org/10.1029/2019JD031059

Shah, H. L., Zhou, T., Huang, M., & Mishra, V. (2019). Strong Influence of Irrigation on Water Budget and Land Surface Temperature in Indian Subcontinental River Basins. *Journal of Geophysical Research: Atmospheres*, *124*(3), 1449–1462. https://doi.org/10.1029/2018JD029132

Shankar, V., Hari Prasad, K. S., Ojha, C. S. P., & Govindaraju, R. S. (2012). Model for Nonlinear Root Water Uptake Parameter. *Journal of Irrigation and Drainage Engineering*, *138*(10), 905–917. https://doi.org/10.1061/(asce)ir.1943-4774.0000469

Shukla, S. P., Puma, M. J., & Cook, B. I. (2014). The response of the South Asian Summer Monsoon circulation to intensified irrigation in global climate model simulations. *Climate Dynamics*, *42*(1–2), 21–36. https://doi.org/10.1007/s00382-013-1786-9

Siebert, S., & Döll, P. (2010). Quantifying blue and green virtual water contents in global crop production as well as potential production losses without irrigation. *Journal of Hydrology*, *384*(3–4), 198–217. https://doi.org/10.1016/j.jhydrol.2009.07.031

Siebert, S., Kummu, M., Porkka, M., Döll, P., Ramankutty, N., & Scanlon, B. R. (2015). A global data set of the extent of irrigated land from 1900 to 2005. *Hydrology and Earth System Sciences*, *19*, 1521–1545. https://doi.org/10.13019/M20599

Sood, N., Gupta, P. K., Srivastava, R. K., & Gosal, S. S. (2006). Comparative studies on field performance of micropropagated and conventionally propagated sugarcane plants. *Plant Tissue Culture and Biotechnology*, *16*(1), 25–29. https://doi.org/10.3329/ptcb.v16i1.1102

Sorooshian, S., Aghakouchak, A., & Li, J. (2014). Influence of irrigation on land hydrological processes over California Soroosh. *Journal of Geophysical Research: Atmospheres*, 1–16. https://doi.org/10.1002/2014JD022232.Received

Srichandan, S., & Mangaraj, A. K. (2015). Growth , Yield and Yield Attributes of Pigeon Pea in Rainfed Uplands of Western Central Table Land Zone of Odisha. *International Journal of Research in Agriculture and Forestry*, *2*(9), 10–13.

Srivastava, A., Rajeevan, M., & Kshirsagar, S. (2009). Development of a high resolution daily gridded temperature data set (1969 – 2005) for the Indian region. *Atmospheric Science Letters*, *10*(October), 249–254. https://doi.org/10.1002/asl

Sulla-Menashe, D., Gray, J. M., Abercrombie, S. P., & Friedl, M. A. (2019). Hierarchical mapping of annual global land cover 2001 to present: The MODIS Collection 6 Land Cover product. *Remote Sensing of Environment*, *222*(December 2018), 183–194. https://doi.org/10.1016/j.rse.2018.12.013

Szilagyi, J., & Jozsa, J. (2018). Evapotranspiration Trends (1979–2015) in the Central Valley of California, USA: Contrasting Tendencies During 1981–2007. *Water Resources Research*, *54*(8), 5620–5635. https://doi.org/10.1029/2018WR022704

Tatsumi, K., & Yamashiki, Y. (2015). Effect of irrigation water withdrawals on water and energy balance in the Mekong River Basin using an improved VIC land surface model with fewer calibration parameters. *Agricultural Water Management*, *159*, 92–106. https://doi.org/10.1016/j.agwat.2015.05.011

Thiery, W., Davin, E. L., Lawrence, D. M., Hirsch, A. L., Hauser, M., & Seneviratne, S. I. (2017). Present-day irrigation mitigates heat extremes. *Journal of Geophysical Research*, *122*(3), 1403–1422. https://doi.org/10.1002/2016JD025740

Thiery, W., Visser, A. J., Fischer, E. M., Hauser, M., Hirsch, A. L., Lawrence, D. M., et al. (2020). Warming of hot extremes alleviated by expanding irrigation. *Nature Communications*, *11*(1), 1–7. https://doi.org/10.1038/s41467-019-14075-4

Tsuchiya, R., Kato, T., & Jeong, J. (2016). Development of SWAT-PADDY for Simulating Lowland Paddy Fields, (November), 1–18. https://doi.org/10.20944/preprints201611.0024.v1

Tsuchiya, R., Kato, T., Jeong, J., & Arnold, J. G. (2018). Development of SWAT-Paddy for Simulating Lowland Paddy Fields. *Sustainability*, *10*(3246). https://doi.org/10.3390/su10093246

Vatta, K., Sidhu, R. S., Lall, U., Birthal, P. S., Taneja, G., Kaur, B., et al. (2018). Assessing the economic impact of a low-cost water-saving irrigation technology in Indian Punjab: the tensiometer. *Water International*, *43*(2), 305–321. https://doi.org/10.1080/02508060.2017.1416443

Verma, D., Gontia, A. S., Jha, A., & Deshmukh, A. (2016). Study on leaf area index and leaf area duration of growth analytical parameters in Wheat, Barley, and Oat. *International Journal of Agriculture, Environment and Biotechnology*, *9*(5), 827. https://doi.org/10.5958/2230-732x.2016.00106.6

Wei, J., Dirmeyer, P. A., Wisser, D., Bosilovich, M. G., & Mocko, D. M. (2013). Where does the irrigation water go? An estimate of the contribution of irrigation to precipitation using MERRA. *Journal of Hydrometeorology*, *14*(1), 275–289. https://doi.org/10.1175/JHM-D-12-079.1

Xie, H., Longuevergne, L., Ringler, C., & Scanlon, B. R. (2020). Integrating groundwater irrigation into hydrological simulation of India: Case of improving model representation of anthropogenic water use impact using GRACE. *Journal of Hydrology: Regional Studies*, *29*(July 2019), 100681. https://doi.org/10.1016/j.ejrh.2020.100681

Xie, X., & Cui, Y. (2011). Development and test of SWAT for modeling hydrological processes in irrigation districts with paddy rice. *Journal of Hydrology*, *396*(1–2), 61–71. https://doi.org/10.1016/j.jhydrol.2010.10.032

Yang, Q., Huang, X., & Tang, Q. (2020). Irrigation cooling effect on land surface temperature across China based on satellite observations. *Science of the Total Environment*, *705*, 135984. https://doi.org/10.1016/j.scitotenv.2019.135984

Zaveri, E., Grogan, D. S., Fisher-Vanden, K., Frolking, S., Lammers, R. B., Wrenn, D. H., et al. (2016). Invisible water, visible impact: Groundwater use and Indian agriculture under climate change. *Environmental Research Letters*, *11*(8). https://doi.org/10.1088/1748-9326/11/8/084005

Zhang, X., Xiong, Z., & Tang, Q. (2017). Modeled effects of irrigation on surface climate in the Heihe River Basin, Northwest China. *Journal of Geophysical Research*, *122*(15), 7881–7895. https://doi.org/10.1002/2017JD026732

Zhengyang, Z., Xinming, M., Guoshun, L., Fangfang, J., Hongbo, Q., Yingwu, Z., et al. (2011). A study on hyperspectral estimating models of tobacco leaf area index. *African Journal of Agricultural Research*, *6*(2), 289–295. https://doi.org/10.5897/AJAR10.533

Zou, M., Niu, J., Kang, S., Li, X., & Lu, H. (2017). The contribution of human agricultural activities to increasing evapotranspiration is significantly greater than climate change effect over Heihe agricultural region. *Scientific Reports*, *7*(1), 1–14. https://doi.org/10.1038/s41598-017-08952-5